

# Optical clocks based on the $\text{Cf}^{15+}$ and $\text{Cf}^{17+}$ ions

S. G. Porsev<sup>1,2</sup>, U. I. Safronova<sup>3</sup>, M. S. Safronova<sup>1,4</sup>, P. O. Schmidt<sup>5,6</sup>, A. I. Bondarev<sup>2,7</sup>, M. G. Kozlov<sup>2,8</sup>, and I. I. Tupitsyn<sup>2,9</sup>

<sup>1</sup>*Department of Physics and Astronomy, University of Delaware, Newark, Delaware 19716, USA*

<sup>2</sup>*Petersburg Nuclear Physics Institute of NRC “Kurchatov Institute”, Gatchina, Leningrad District, 188300, Russia,*

<sup>3</sup>*Physics Department, University of Nevada, Reno, Nevada 89557, USA*

<sup>4</sup>*Joint Quantum Institute, National Institute of Standards and Technology and the University of Maryland, College Park, Maryland 20742, USA*

<sup>5</sup>*Physikalisch-Technische Bundesanstalt, Bundesallee 100, 38116 Braunschweig, Germany*

<sup>6</sup>*Institut für Quantenoptik, Leibniz Universität Hannover, Welfengarten 1, 30167 Hannover, Germany*

<sup>7</sup>*Center for Advanced Studies, Peter the Great St. Petersburg Polytechnic University, Polytechnicheskaya 29, St. Petersburg, 195251, Russia*

<sup>8</sup>*St. Petersburg Electrotechnical University LETI,*

*Prof. Popov Str. 5, St. Petersburg, 197376, Russia*

<sup>9</sup>*Department of Physics, St. Petersburg State University,*

*Ulianovskaya 1, Petrodvorets, St. Petersburg, 198504, Russia*

(Dated: April 14, 2020)

Recent experimental progress in cooling, trapping, and quantum logic spectroscopy of highly-charged ions (HCIs) made HCIs accessible for high resolution spectroscopy and precision fundamental studies. Based on these achievements, we explore a possibility to develop optical clocks using transitions between the ground and a low-lying excited state in the  $\text{Cf}^{15+}$  and  $\text{Cf}^{17+}$  ions. Using a high-accuracy relativistic method of calculation we predicted the wavelengths of clock transitions, calculated relevant atomic properties, and analyzed a number of systematic effects (such as the electric quadrupole-, micromotion-, and quadratic Zeeman shifts of the clock transitions) that affect the accuracy and stability of the optical clocks. We also calculated magnetic dipole hyperfine-structure constants of the clock states and the blackbody radiation shifts of the clock transitions.

## I. INTRODUCTION

Recent years marked a rapid development of both highly-charged ion (HCI) theory and experiment. An experimental progress in cooling and trapping of HCIs using sympathetic cooling made them accessible for high resolution spectroscopy and precision fundamental studies [1–3].

The pioneering works of Schiller [4] and Berengut *et al.* [5] proposed to use optical transitions in HCIs for frequency metrology and tests for a variation of the fundamental constants. In a number of subsequent theoretical studies (see recent review [2] and references therein) it was demonstrated that a number of HCIs have narrow transitions lying in the optical frequency range, which can be used for developing high-accuracy clocks as well as other properties desirable for precision frequency metrology.

In comparison to neutral atoms, HCIs have several advantages. They have a more compact size and, hence, are less sensitive to external electric field perturbations. Preliminary estimates of a systematic uncertainty that can be obtained using shift mitigation and cancellation strategies suggest that the uncertainties well below  $10^{-18}$  may be achievable [6–8]. The sensitivity of an HCI clock transition to a variation of the fine-structure constant  $\alpha$  is expected to be higher than in neutral atoms as a consequence of strong relativistic effects and high ionization energies [5]. Such a sensitivity to  $\alpha$  variation is essential to search for hypothetical oscillations and occasional jumps of  $\alpha$  due to topological defects [9] and cosmological

fields, including dark matter [10, 11].

The theoretical efforts were supported by the development of experimental techniques allowing to decelerate, trap, cool, and control HCIs. It was demonstrated that HCIs produced in an electron beam ion trap (EBIT) can be ejected, decelerated, and stopped inside of a Coulomb crystal of laser-cooled  $\text{Be}^+$  ions confined in a cryogenic Paul trap [12, 13]. Sympathetic cooling allowed to decrease the temperature of HCIs to a mK regime [1]. The sympathetic cooling of a single  $\text{Ar}^{13+}$  to the motional ground state was demonstrated in a new cryogenic Paul trap experiment at PTB [14, 15]. In 2020, coherent laser spectroscopy of highly charged  $^{40}\text{Ar}^{13+}$  using quantum logic was demonstrated, achieving an increase in precision of HCI frequency measurement by eight orders of magnitude [3].

In this work we explore a possibility to develop optical clocks using the transitions between the ground and a low-lying excited state of the highly-charged  $\text{Cf}^{15+}$  and  $\text{Cf}^{17+}$  ions. Three out of eight main Cf isotopes have a long half-life:  $A = 249, I = 9/2$  (351 y),  $A = 250, I = 0$  (13.1 y), and  $A = 251, I = 1/2$  (898 y), where  $A$  is the number of nucleons and  $I$  is the nuclear spin.

Both  $\text{Cf}^{15+}$  and  $\text{Cf}^{17+}$  ions have the  $[1s^2, \dots, 5d^{10}, 6s^2]$  core. The former,  $\text{Cf}^{15+}$ , is a Bi-like ion with three valence electrons above the core, while  $\text{Cf}^{17+}$  has one valence electron above the core, allowing to consider it as a univalent element. But as a detailed analysis shows, more correct and accurate results are obtained if we consider  $\text{Cf}^{17+}$  as a trivalent ion including both  $6s$  electrons into the valence field. This is particular important for

correct determination of lowest-lying even-parity energy levels whose main configuration, according to our calculation, is  $(6s5f^2)$ , i.e., it contains unpaired  $6s$  electron.

Both the  $\text{Cf}^{17+}$  and  $\text{Cf}^{15+}$  ions were studied previously in Refs. [16, 17] and found to be particularly good candidates for testing variation of the fine-structure constant. The calculation carried out in [17] identified the ground and first excited state of  $\text{Cf}^{15+}$  as the states with a high sensitivity to  $\alpha$  variation and convenient clock wavelength. The dimensionless sensitivity factor  $|\Delta K|$  to a variation of  $\alpha$  for the  $\text{Cf}^{17+}$  and  $\text{Cf}^{15+}$  clock pair was predicted to be 107 (see [2]), while the largest  $|\Delta K|$  factor for any of the currently operating clock pair is 7 (for E3/E2 transitions in  $\text{Yb}^+$ ) and most are below 1.

This paper is a guide for future experimental work, providing a detailed assessment of both ions for the clock development missing so far for most of the suggested HCI clock candidates, as noted in the recent review [2]. In Sections II and III we briefly describe the method of calculation and discuss the properties of the low-lying states, such as energies, lifetimes, and transition wavelengths. In Section IV we explore a number of systematic effects, such as the electric quadrupole-, micromotion-, and quadratic Zeeman shifts of the clock transitions, which affect the accuracy of optical clocks. We also present the results of calculation of the magnetic dipole hyperfine-structure (hfs) constants of the clock states and the black-body radiation (BBR) shifts of the clock transitions. The final section contains concluding remarks.

## II. METHOD OF CALCULATION

We consider  $\text{Cf}^{15+}$  and  $\text{Cf}^{17+}$  as the ions with three valence electrons above closed cores  $[1s^2, \dots, 5d^{10}6s^2]$  and  $[1s^2, \dots, 5d^{10}]$ , respectively. We start from solution of the Dirac-Hartree-Fock (DHF) equations in the  $V^{N-3}$  approximation for both ions, where  $N$  is the total number of electrons. The initial self-consistency procedure was carried out for the core electrons and then the  $5f$ ,  $6p$ ,  $6d$ ,  $7s$ , and  $7p$  orbitals (and also  $6s$  in case of  $\text{Cf}^{17+}$ ) were constructed in the frozen-core potential. The remaining virtual orbitals were formed using a recurrent procedure described in [18]. For both ions, the basis sets included in total 7 partial waves ( $l_{\text{max}} = 6$ ) and orbitals with principal quantum number  $n$  up to 25. We included the Breit interaction on the same footing as the Coulomb interaction at the stage of constructing the basis set. QED corrections were also included following Ref. [19, 20].

We use a hybrid approach combining configuration interaction (CI) (that takes into account an interaction between valence electrons) and a method accounting for core-valence correlations [21, 22]. The wave functions and energy levels of the valence electrons were found by solving the multiparticle relativistic equation [21],

$$H_{\text{eff}}(E_n)\Phi_n = E_n\Phi_n, \quad (1)$$

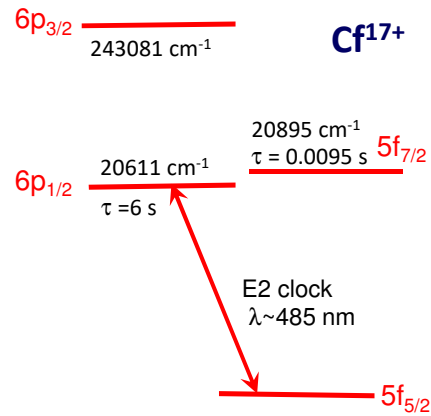


FIG. 1. The level scheme for low-lying odd-parity levels of  $\text{Cf}^{17+}$ .

where the effective Hamiltonian is defined as

$$H_{\text{eff}}(E) = H_{\text{FC}} + \Sigma(E), \quad (2)$$

with  $H_{\text{FC}}$  being the Hamiltonian in the frozen-core approximation. The energy-dependent operator  $\Sigma(E)$  accounts for virtual excitations of the core electrons. We constructed it in three ways: using (i) the second-order many-body perturbation theory (MBPT) over residual Coulomb interaction [21], (ii) the linearized coupled cluster single-double (LCCSD) method [22, 23], and (iii) the coupled cluster single double (valence) triple (CCSDT) method. In the last case, using the expressions for cluster amplitudes derived in [24], we included the non-linear (NL) terms and valence triple excitations into the formalism of the CI+all-order method developed in Ref. [22]. We note that the equations for the valence triples are solved iteratively. In the following we refer to these approaches, as the CI+MBPT, CI+LCCSD, and CI+CCSDT methods.

The sets of  $\text{Cf}^{15+}$  configurations for the odd- and even-parity states were constructed by allowing single and double excitations from the  $5f6p^2$  and  $5f^26p$  configurations and from the  $6p^26d$ ,  $5f6p6d$  and  $5f^26d$  configurations, respectively, to  $7-20s$ ,  $7-20p$ ,  $7-20d$ ,  $6-19f$ , and  $5-13g$  shells (we designate it as  $[20spd19f13g]$ ). The sets of  $\text{Cf}^{17+}$  configurations for the odd- and even-parity states were formed allowing single and double excitations from the  $6s^25f$  and  $6s^26p$  and from the  $6s5f^2$  and  $6s5f6p$  configurations, respectively, to  $[20spd19f13g]$ . We checked for both ions that if we allowed the single and double excitations to higher lying  $f$  and  $g$  shells and also triple excitations from the main configurations, the energies (counted from the ground state) changed only by few tens  $\text{cm}^{-1}$ .

The level schemes for low-lying levels of  $\text{Cf}^{17+}$  and  $\text{Cf}^{15+}$  are given in Fig. 1 and Fig. 2.

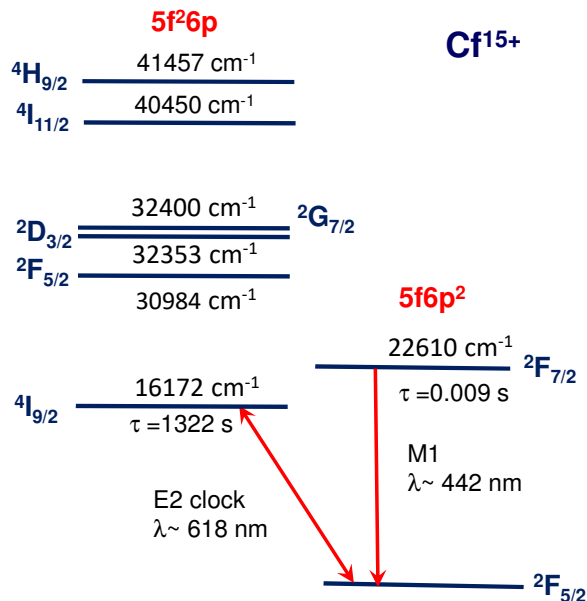


FIG. 2. The level scheme for low-lying levels of  $\text{Cf}^{15+}$ .

### III. ENERGY LEVELS

The energies of the lowest-lying states of  $\text{Cf}^{15+}$  and  $\text{Cf}^{17+}$  obtained in different approximations are listed in Table I. The energies of the excited states (in  $\text{cm}^{-1}$ ) are counted from the ground state. The assignments of the  $\text{Cf}^{15+}$  odd levels are from Ref. [17]. For designation of all other terms we use the main configuration and the total angular momentum  $J$  of the state as a subscript.

In the third and forth columns we present the pure CI and CI+MBPT values. Contributions from higher-order (HO) correlations (difference of the CI+LCCSD and CI+MBPT calculations) and from the NL terms and triple excitations (difference of the CI+CCSDT and CI+LCCSD calculations) are given separately in columns labeled “HO” and “NLTr”. Following an empiric rule obtained for Ag-like ions in Ref. [25] and applied for Cd-like and Sn-like ions in Ref. [26] we estimate the contribution of the higher ( $l > 6$ ) partial waves as the contribution of the  $l = 6$  partial wave obtained as the difference of two calculations where all intermediate sums in the all-order and MBPT terms are restricted to  $l_{\text{max}} = 6$  and  $l_{\text{max}} = 5$ . This contribution is listed in Table I in column labeled “Extrap”. The final theoretical results, listed in the “Final??” column, are obtained as the sum of the CI+MBPT values and HO, NLTr, and Extrap corrections.

We find that the clock transition energies between the ground and first excited state are very sensitive to different corrections for both ions. The CI+MBPT value differs from the CI value by more than a factor of 2 for both ions, i.e., the contribution of the core-valence correlation corrections is as large as the CI result. An inclusion of the HO corrections, the NL terms and valence triples in the framework of the CI+LCCSD and CI+CCSDT meth-

ods further changed the energies by several thousands of  $\text{cm}^{-1}$ .

The  $\text{Cf}^{15+}$  clock transition energy found at the CI+LCCSD stage is in a reasonable agreement with the results of Refs. [17, 20]. The quadratic NL terms and valence triples, contributing  $3675 \text{ cm}^{-1}$  to the transition energy, were not taken into account in [17, 20], what explains a difference between the present result and the clock transition energy predicted in those works. Taking into account an importance of the NL terms and valence triple excitations and also noting that the present calculation still omits the core triples and higher-order NL terms, we estimate the uncertainty of the clock transition energies as a half of difference between the CI+CCSDT and CI+LCCSD values.

This conservative estimate is based on a conclusion drawn from calculations for Na [27] and Cs [28] that the contribution from the valence triples and NL terms is (much) larger than the contribution from core triples. Thus, the uncertainty of the clock transition energy is  $\sim 1800 \text{ cm}^{-1}$  for  $\text{Cf}^{15+}$  and  $\sim 600 \text{ cm}^{-1}$  for  $\text{Cf}^{17+}$ . Taking these uncertainties into account we neglect corrections to the transition energies due to effective three-particle interactions between valence electrons. These corrections were found to be at the level of  $100 \text{ cm}^{-1}$  or less for the low-lying states of  $\text{Cf}^{15+}$  [20].

In Table II we present the wavelengths between the ground and excited states (in nm) and the excited states lifetimes (in s) for  $\text{Cf}^{15+}$  and  $\text{Cf}^{17+}$  obtained in the CI+CCSDT approximation and compare with other calculations where available. The  $\text{Cf}^{15+}$  first excited state,  $5f^2 6p \ ^4I_{9/2}^o$ , has a rather long lifetime, 22 min. This is because it decays to the ground state through a weak  $E2$  transition. Our predicted lifetime of the  $^4I_{9/2}^o$  state is 5 times smaller than the value obtained in Ref. [17], mostly due to change in the predicted clock transition energy, since the probability of the  $E2$  transition is proportional to  $(\Delta E)^5$ . The lifetimes of other listed excited states are several orders of magnitude smaller. In particular,  $5f^2 6p \ ^2F_{5/2}^o$  and  $^2F_{7/2}^o$  are the fine-structure levels of the same manifold and there is a relatively strong  $M1 \ ^2F_{7/2}^o - ^2F_{5/2}^o$  transition. The same is true for the  $5f^2 6p \ ^4I_{9/2}^o$  and  $^4I_{11/2}^o$  pair of levels.

For  $\text{Cf}^{17+}$ , the  $6s^2 6p_{1/2}$  clock excited state also decays to the ground state through the  $E2$  transition. The probability of this transition is  $0.17 \text{ s}^{-1}$  leading to the lifetime of this state,  $\tau \approx 6.0 \text{ s}$ . We note that the probability of the  $M3 \ 6s^2 6p_{1/2} - 6s^2 5f_{7/2}$  transition is negligible.

### IV. SYSTEMATIC EFFECTS

In this section we consider a number of systematic effects relevant to the clock  $5f^2 6p \ ^4I_{9/2}^o - 5f 6p^2 \ ^2F_{5/2}^o$  and  $6s^2 6p_{1/2} - 6s^2 5f_{5/2}$  transitions in  $\text{Cf}^{15+}$  and  $\text{Cf}^{17+}$ , respectively. We use wave functions obtained in the CI+CCSDT approximation in all subsequent calculations

TABLE I. The energies of the excited states (in  $\text{cm}^{-1}$ ), counted from the ground state, calculated in the CI and CI+MBPT approximations. Contributions from higher-order (HO) correlations (difference of the CI+LCCSD and CI+MBPT calculations) and from the NL terms and triple excitations (difference of the CI+CCSDT and CI+LCCSD calculations) and estimated contributions of higher partial waves ( $l > 6$ ) are given separately in columns HO, NLTr, and Extrap. The final values, given in the column labeled “Final”, are obtained as the sum of the CI+MBPT values and HO, NLTr, and Extrap corrections. We use the main configuration and the total angular momentum  $J$  as a subscript to designate the  $\text{Cf}^{15+}$  even-parity levels and the levels of  $\text{Cf}^{17+}$ .

	Level	CI	CI+MBPT	HO	NLTr	Extrap	Final	Ref. [16]	Ref. [20]	Ref. [17]
$\text{Cf}^{15+}$	$5f6p^2\ ^2F_{5/2}^o$	0	0	0	0	0	0		0	0
	$5f^26p\ ^4I_{9/2}^o$	28930	10549	2907	3675	-959	16172		12898	12314
	$5f6p^2\ ^2F_{7/2}^o$	22269	22388	-107	486	-158	22610		22018	21947
	$5f^26p\ ^2F_{5/2}^o$	43441	25803	2242	3741	-802	30984		27127	26665
	$5f^26p\ ^2D_{3/2}^o$	45515	26984	2483	3855	-969	32353			27750
	$5f^26p\ ^2G_{7/2}^o$	43552	28809	1276	3081	-765	32400		29214	28875
	$5f^26p\ ^4I_{11/2}^o$	51995	35979	1715	3717	-961	40450		37081	36564
	$5f^26p\ ^4H_{9/2}^o$	52793	37304	1522	3564	-934	41457		37901	37392
	$(6p^26d)_{3/2}$	520444	544228	-3419	-4383	1089	537515			
	$(5f6p6d)_{9/2}$	534519	545581	-1612	-2445	249	541773			
	$(5f6p6d)_{7/2}$	538082	548797	-1634	-2152	235	545245			
	$(5f6p6d)_{5/2}$	538863	549387	-1508	-2156	216	545939			
	$(5f6p6d)_{3/2}$	547123	556562	-1207	-1907	190	553637			
	$\text{Cf}^{17+}$	$(6s^2\ 5f)_{5/2}^o$	0	0	0	0	0	0	0	
$(6s^2\ 6p)_{1/2}^o$		10104	22118	-1402	-1126	1021	20611	18686		
$(6s^2\ 5f)_{7/2}^o$		19682	22116	-1102	-152	33	20895	21848		
$(6s^2\ 6p)_{3/2}^o$		228778	245070	-1783	-1341	1136	243081	242811		
$(6s\ 5f^2)_{7/2}$		206421	202671	-496	-340	-945	200890			
$(6s\ 5f^2)_{9/2}$		211719	208829	-707	-415	-942	206765			
$(6s\ 5f^2)_{3/2}$		212749	210608	-860	-414	-833	208501			
$(6s\ 5f^2)_{5/2}$		219342	213728	-1663	-1524	-359	210182			
$(6s\ 5f\ 6p)_{5/2}$		206500	220621	-1855	-1252	-463	217050			

TABLE II. The wavelengths between the ground and excited states (in nm) and the excited states lifetimes (in s).

	Level	This work		Ref. [17]	
		$\lambda(\text{nm})$	$\tau(\text{s})$	$\lambda(\text{nm})$	$\tau(\text{s})$
$\text{Cf}^{15+}$	$5f6p^2\ ^2F_{5/2}^o$	0		0	0
	$5f^26p\ ^4I_{9/2}^o$	618	1322	812	6900
	$5f6p^2\ ^2F_{7/2}^o$	442	0.009	456	0.012
	$5f^26p\ ^2F_{5/2}^o$	323	0.18	375	0.26
	$5f^26p\ ^4I_{11/2}^o$	247	0.003	273	0.003
$\text{Cf}^{17+}$	$(6s^2\ 5f)_{5/2}^o$	0			
	$(6s^2\ 6p)_{1/2}^o$	485	6.0		
	$(6s^2\ 5f)_{7/2}^o$	479	0.0095		
	$(6s^2\ 6p)_{3/2}^o$	41	$7 \times 10^{-6}$		

for both ions. We also simplify notation for the  $\text{Cf}^{17+}$  clock states as  $6s^2\ 5f_{5/2} \equiv 5f_{5/2}$  and  $6s^2\ 6p_{1/2} \equiv 6p_{1/2}$ . In calculating matrix elements (MEs) of different operators the random phase approximation (RPA) corrections were included.

### A. Electric quadrupole shift

The Hamiltonian,  $H_Q$ , describing the interaction of the external electric-field gradient with the quadrupole moment of an atomic state  $|\gamma JIFM\rangle$  (where  $J$  is the total angular momentum of the electrons,  $I$  is the nuclear spin,  $\mathbf{F} = \mathbf{J} + \mathbf{I}$ ,  $M$  is the projection of  $\mathbf{F}$ , and  $\gamma$  encapsulates all other electronic quantum numbers) is given by

$$H_Q = \sum_{q=-2}^2 (-1)^q \nabla \mathcal{E}_q^{(2)} Q_{-q}, \quad (3)$$

where the  $q = 0$  component of  $\nabla \mathcal{E}^{(2)}$  can be written as [29, 30]:

$$\nabla \mathcal{E}_0^{(2)} = -\frac{1}{2} \frac{\partial \mathcal{E}_z}{\partial z}. \quad (4)$$

Coupling of this field gradient to the quadrupole moment of the atomic state leads to the energy shift:

$$\Delta E = -\frac{1}{2} \langle Q_0 \rangle \frac{\partial \mathcal{E}_z}{\partial z}, \quad (5)$$

where  $\langle Q_0 \rangle \equiv \langle \gamma JIFM | Q_0 | \gamma JIFM \rangle$ .

The fractional electric quadrupole shift of the clock transition is then

$$\frac{\Delta\nu}{\nu_{\text{clock}}} = -\frac{1}{2h\nu_{\text{clock}}} \Delta\langle Q_0 \rangle \frac{\partial \mathcal{E}_z}{\partial z}, \quad (6)$$

where  $\nu_{\text{clock}}$  is the clock transition frequency,  $h$  is the Planck constant, and  $\Delta\langle Q_0 \rangle$  is the difference of the expectation values of  $Q_0$  for the upper and lower clock states.

The ME  $\langle \gamma JIFM | Q_0 | \gamma JIFM \rangle$  can be written as

$$\begin{aligned} \langle \gamma JIFM | Q_0 | \gamma JIFM \rangle &= (-1)^{I+J+F} \\ &\times [3M^2 - F(F+1)] \sqrt{\frac{2F+1}{(2F+3)(F+1)F(2F-1)}} \\ &\times \left\{ \begin{matrix} J & 2 & J \\ F & I & F \end{matrix} \right\} \langle \gamma J || Q || \gamma J \rangle, \end{aligned} \quad (7)$$

where  $\langle \gamma J || Q || \gamma J \rangle$  is the reduced ME of the electric quadrupole operator.

Our calculation gives

$$\begin{aligned} \langle {}^2F_{5/2}^o || Q || {}^2F_{5/2}^o \rangle &\approx 0.31 |e| a_0^2, \\ \langle {}^4I_{9/2}^o || Q || {}^4I_{9/2}^o \rangle &\approx 0.53 |e| a_0^2, \end{aligned} \quad (8)$$

for the ground and first excited states of  $\text{Cf}^{15+}$ , where  $e$  is the electron charge and  $a_0$  is the Bohr radius.

Using these MEs and the expression for the quadrupole moment  $\Theta$  of an atomic state  $|\gamma J\rangle$  given by

$$\begin{aligned} \Theta &= 2 \langle \gamma J, M_J = J | Q_0 | \gamma J, M_J = J \rangle \\ &= 2 \sqrt{\frac{J(2J-1)}{(2J+3)(J+1)(2J+1)}} \langle \gamma J || Q || \gamma J \rangle \end{aligned} \quad (9)$$

we can find the quadrupole moments of the clock states to be

$$\begin{aligned} \Theta({}^2F_{5/2}^o) &\approx 0.15 |e| a_0^2, \\ \Theta({}^4I_{9/2}^o) &\approx 0.25 |e| a_0^2. \end{aligned} \quad (10)$$

As follows from Eq. (7), the quadrupole shift turns to zero when  $3M^2 = F(F+1)$ . For both fermionic 249 and 251 isotopes of Cf with  $I = 9/2$  and  $I = 1/2$ , there are sublevels of the ground state with  $F = 3, M = \pm 2$  for which the quadrupole shift disappears. For the 249 isotope, the total angular momentum  $F$  of the upper clock state ranges from 0 to 9. If we also choose  $F = 3, M = \pm 2$  for this state, the clock transition is not affected by the quadrupole shift. Averaging over the  $M = \pm 2$  transitions furthermore eliminates the linear Zeeman shift. For the 251 isotope, the upper state total angular momentum  $F$  can be equal to 4 or 5. Averaging over all pairs of  $\pm|M|$  in this excited state will make the difference  $3M^2 - F(F+1)$  vanish to suppress the electric quadrupole shift [31].

In general, as follows from Eq. (7),

$$\sum_M \langle \gamma JIFM | Q_0 | \gamma JIFM \rangle = 0, \quad (11)$$

and the same is true for the  $H_Q$  operator given by Eq. (3) [30]. Thus, the quadrupole shift vanishes when averaged over all  $M$ . This technique has been employed in singly-charged frequency standards [32–34] to suppress the uncertainty in this shift by up to four orders of magnitude [35].

To get an upper limit for the quadrupole shift we put  $M = 0$  in Eq. (7) and chose such values of  $F$  for the upper and lower clock states to maximize  $|\Delta\langle Q_0 \rangle|$ . It gives us  $|\Delta\langle Q_0 \rangle| \sim 0.1 |e| a_0^2$ . Substituting it into Eq. (6) and using for an estimate  $\partial \mathcal{E}_z / \partial z \approx 1 \text{ kV/cm}^2 \approx 1.029 \times 10^{-15} \text{ a.u.}$ , we obtain for the quadrupole shift:

$$\frac{\Delta\nu}{\nu_{\text{clock}}} \simeq 7 \times 10^{-16}. \quad (12)$$

Even in this (worst) case, a 3-4 order of magnitude suppression will make the electric quadrupole shift well below  $10^{-18}$ .

For  $\text{Cf}^{17+}$ , the quadrupole moment of the upper clock state  $6p_{1/2}$  is equal to 0. For the ground  $5f_{5/2}$  state we obtain

$$\begin{aligned} \langle 5f_{5/2} || Q || 5f_{5/2} \rangle &\approx 0.80 |e| a_0^2, \\ \Theta(5f_{5/2}) &\approx 0.39 |e| a_0^2. \end{aligned} \quad (13)$$

For both 249 and 251 isotopes there is the sublevel of the ground state with  $F = 3, M = \pm 2$  for which the quadrupole shift vanishes. As a result, it vanishes also for the clock transition.

We can compare these results with those obtained for  $\text{Sr}^+$  where the suppression technique discussed above was applied. Using the recent measurement of the electric quadrupole moment of the  $\text{Sr}^+ 4d_{5/2}$  clock state [36] and noting that our definition of the quadrupole moment differs by factor of 2 from that used in Ref. [36], we obtain  $|\langle 4d_{5/2} || Q || 4d_{5/2} \rangle| \approx 10.7 |e| a_0^2$ . This value is more than an order of magnitude larger than the respective MEs for  $\text{Cf}^{15+}$  and  $\text{Cf}^{17+}$  given by Eqs. (8) and (13).

## B. Black-body radiation shift

A BBR shift of the clock energy levels is due to an interaction of thermal photons with the atom. The fractional shift of the clock transition is given by

$$\begin{aligned} \frac{\Delta\nu_{\text{BBR}}}{\nu_{\text{clock}}} &\approx -\frac{\pi^2}{15 c^3 \hbar^4} \frac{\Delta\alpha}{\nu_{\text{clock}}} (k_B T)^4 \\ &\equiv \beta_{\text{BBR}} \left( \frac{T}{300 \text{ K}} \right)^4, \end{aligned} \quad (14)$$

where  $\Delta\alpha \equiv \alpha({}^4I_{9/2}^o) - \alpha({}^2F_{5/2}^o)$  for  $\text{Cf}^{15+}$  and  $\Delta\alpha \equiv \alpha(6p_{1/2}) - \alpha(5f_{5/2})$  for  $\text{Cf}^{17+}$  are the differential scalar static polarizabilities,  $c$  is the speed of light,  $k_B$  is the Boltzmann constant, and  $T$  is the BBR temperature.

We can present the scalar polarizability  $\alpha$  as a sum of the valence polarizability,  $\alpha_v$ , ionic-core polarizability

$\alpha_c$ , and a small term  $\alpha_{vc}$  that modifies ionic-core polarizability due to the presence of valence electrons:

$$\alpha = \alpha_v + \alpha_c + \alpha_{vc}. \quad (15)$$

The valence part of the scalar static polarizability of a state  $|0\rangle$  with the energy  $E_0$  and total angular momentum  $J_0$  is determined as

$$\alpha_0^v = \frac{2}{3(2J_0 + 1)} \sum_n \frac{|\langle 0 || D || n \rangle|^2}{E_n - E_0}, \quad (16)$$

where  $\mathbf{D}$  is the electric-dipole operator. Instead of direct summation over all intermediate states we solve the inhomogeneous equation in the valence space [37]:

$$(E_0 - H_{\text{eff}})|\psi\rangle = D_z|0\rangle \quad (17)$$

and then use  $|\psi\rangle$  to find  $\alpha_0^v$ . The core and  $vc$  terms are evaluated in the single-particle approximation including RPA [38];  $\alpha_{vc}$  are calculated by adding  $vc$  contributions from individual electrons. Thus, for  $\text{Cf}^{15+}$ ,  $\alpha_{vc}(^2F_{5/2}^o) = \alpha_{vc}(5f_{5/2}) + 2\alpha_{vc}(6p_{1/2})$  and  $\alpha_{vc}(^4I_{9/2}^o) = 2\alpha_{vc}(5f_{5/2}) + \alpha_{vc}(6p_{1/2})$ .

The results of calculation of the scalar static polarizabilities and the parameters  $\beta_{\text{BBR}}$  are given in Table III. Only the valence polarizabilities  $\alpha_v$  were found in Ref. [17]; these results are in a reasonable agreement with our values for  $\alpha_v$ . We would like to note an enhanced role of the  $vc$  terms for  $\text{Cf}^{15+}$ . While the core contribution cancels in the differential polarizability, the  $vc$  term does not. It nearly cancels the valence polarizability and significantly affects the result.

The differential polarizabilities,  $\Delta\alpha$ , are very small for both ions leading to small values of the static BBR shifts (we neglect dynamic corrections to them). We note that for both ions, the scalar static polarizabilities of the clock states are close in magnitude and by an order of magnitude (in absolute value) larger than  $\Delta\alpha$ . As a result the uncertainty of the differential polarizabilities is large. For instance for  $\text{Cf}^{17+}$ , if  $\alpha(6p_{1/2})$  is increased by 1% while  $\alpha(5f_{5/2})$  is reduced by 1%,  $\Delta\alpha$  will change by a factor of 2. Thus, one should consider the values of the differential polarizabilities as estimates.

The BBR shifts of the  $\text{Cf}^{15+}$  and  $\text{Cf}^{17+}$  clock transitions of the order of  $10^{-18}$  even at  $T = 300$  K. Since the highly-charged ion trap is operated at cryogenic temperature near  $T = 4$  K [2] the BBR shifts for both ions will be suppressed by more than 7 orders of magnitude, even compared to small room temperature values, making them negligible.

### C. Micromotion shift

A micromotion driven by the rf-trapping field leads to ac Stark and second-order Doppler shifts. As it was shown in [35], if  $\Delta\alpha$  for the clock transition is negative,

TABLE III. Contributions  $\alpha_v$ ,  $\alpha_c$ , and  $\alpha_{vc}$  to the scalar static polarizabilities of the clock states, the differential polarizabilities  $\Delta\alpha$ , and the parameter  $\beta_{\text{BBR}}$ , determined in the text, are presented.  $\alpha = \alpha_v + \alpha_c + \alpha_{vc}$ .

	State	(in $a_0^3$ )	This work	Ref. [17]
$\text{Cf}^{15+}$	$^2F_{5/2}^o$	$\alpha_v$	0.323	0.317
		$\alpha_c$	0.948	
		$\alpha_{vc}$	-0.381	
		$\alpha$	0.890	
	$^4I_{9/2}^o$	$\alpha_v$	0.245	0.183
		$\alpha_c$	0.948	
		$\alpha_{vc}$	-0.207	
		$\alpha$	0.986	
		$\Delta\alpha$	0.096	-0.134
		$\beta_{\text{BBR}}$	$-1.7 \times 10^{-18}$	$2.9 \times 10^{-18}$
$\text{Cf}^{17+}$	$5f_{5/2}$	$\alpha_v$	0.645	
		$\alpha_c$	0.344	
		$\alpha_{vc}$	-0.028	
		$\alpha$	0.961	
	$6p_{1/2}$	$\alpha_v$	0.595	
		$\alpha_c$	0.344	
		$\alpha_{vc}$	-0.020	
		$\alpha$	0.919	
		$\Delta\alpha$	-0.042	
		$\beta_{\text{BBR}}$	$5.9 \times 10^{-19}$	

there is a “magic” trap drive frequency  $\Omega$  given by

$$\Omega = \frac{|e|}{M_i c} \sqrt{-\frac{h\nu_{\text{clock}}}{\Delta\alpha}} \quad (18)$$

( $M_i$  is the ion mass) at which the micromotion shift vanishes. Substituting  $M_i \approx A m_p$  (where  $m_p$  is the proton mass and we use for an estimate  $A = 251$ ) and the differential polarizability of  $\text{Cf}^{17+}$ ,  $\Delta\alpha = -0.042 a_0^3$ , to Eq. (18), we obtain  $\Omega \approx 2\pi \times 155$  MHz.

For  $\text{Cf}^{15+}$  we obtained positive value of  $\Delta\alpha$  and a “magic” trap drive frequency does not exist. But in this case compensation voltages, allowing to direct the ion back to a position where radio-frequency field vanishes, can be applied [39, 40]. If these voltages are well controlled the excess micromotion does not pose a limitation to optical frequency standards [2].

### D. Hyperfine interaction

We also calculated the magnetic-dipole hfs constants  $A$  for the clock states of the  $\text{Cf}^{15+}$  and  $\text{Cf}^{17+}$  ions.

The nuclear magnetic moment,  $\mu_I$ , is unknown for  $^{251}\text{Cf}$ . For the 249 isotope the results obtained for  $\mu_I$  are somewhat contradictory. The absolute value,  $|\mu_I| = 0.28(6) \mu_N$  (where  $\mu_N$  is the nuclear magneton), was experimentally found in [41] while the theoretical calculation carried out in that work gave  $\mu_I = -0.49 \mu_N$ .

TABLE IV. The values of  $A/g_I$  (in MHz) for the clock states of  $\text{Cf}^{15+}$  and  $\text{Cf}^{17+}$ .

State	$A/g_I$	
$\text{Cf}^{15+}$	$2F_{5/2}^o$	4200
	$4I_{9/2}^o$	21000
$\text{Cf}^{17+}$	$5f_{5/2}$	1900
	$6p_{1/2}$	195000

For this reason, we present our results in the form  $A/g_I$ , keeping the nuclear  $g$  factor,  $g_I \equiv \mu_I/(I\mu_N)$ , as a multiplier. The values of  $A/g_I$ , which are approximately the same for both 249 and 251 isotopes, are listed in Table IV. We estimate the accuracy of these values at the level of 20-30%.

### E. Zeeman shift

In the presence of an external magnetic field  $\mathbf{B}$  atomic energy levels (and transition frequencies) experience the linear and quadratic Zeeman shifts. The former scales linearly with the magnetic quantum number  $M$ . It equals 0 at  $M = 0$  and can be suppressed in other cases if the frequency is averaged over two or more transitions with linear Zeeman shifts equal in absolute value but having the opposite signs [42].

To determine the quadratic Zeeman shift in the case of a weak magnetic field, we have to consider both hyperfine and Zeeman interactions:

$$H = H_{\text{hfs}} - \boldsymbol{\mu}_{\text{at}} \mathbf{B} \quad (19)$$

with  $\boldsymbol{\mu}_{\text{at}} = -\mu_B g_J \mathbf{J} - \mu_N g_I \mathbf{I}$ . Here,  $\mu_B$  is the Bohr magneton and  $g_J$  is the electron  $g$  factor, given in the nonrelativistic approximation by the formula

$$g_J = \frac{3}{2} + \frac{S(S+1) - L(L+1)}{2J(J+1)}. \quad (20)$$

Below, we estimate this effect for  $^{251}\text{Cf}$ , that has the nuclear spin  $I = 1/2$ . In this case,

$$H_{\text{hfs}} = hA \mathbf{I} \mathbf{J}, \quad (21)$$

where  $A$  is the magnetic dipole hyperfine structure constant (in Hz).

If  $I = 1/2$ , the total angular momentum  $F = J \pm 1/2$ . For the case of  $J = 1/2$ ,  $F = I \pm 1/2$ , the resulting energy shift was obtained by Breit and Rabi in Ref. [43]. Following the approach of [43], we obtain for the energy shift

$$\begin{aligned} \Delta E_{F=J\pm 1/2} &= -\frac{h\Delta W}{2(2J+1)} + \mu_B g_J m_F B \\ &\pm \frac{1}{2} \sqrt{(h\Delta W)^2 + \frac{2m_F h\Delta W y}{J+1/2} + y^2}, \end{aligned} \quad (22)$$

where

$$y \equiv (\mu_N g_I - \mu_B g_J) B$$

and  $\Delta W \equiv A(J+1/2)$  is the splitting (in Hz) between two hyperfine sublevels in the absence of the magnetic field.

If the magnetic field is weak,  $B \sim 10^{-5}$  T, then  $|y| \ll h\Delta W$ . It follows from Eq. (22), that the contribution quadratic in  $B$  to  $\Delta E_{F=J\pm 1/2}$  (we designate it as  $\Delta E_{F=J\pm 1/2}^{(2)}$ ) is proportional to  $y^2$  and is given by

$$\Delta E_{F=J\pm 1/2}^{(2)} = \pm \frac{y^2}{4h\Delta W} \approx \pm \frac{1}{2(2J+1)} \frac{(\mu_B g_J)^2}{hA} B^2.$$

For the  $\text{Cf}^{15+}$  clock  $4I_{9/2}^o - 2F_{5/2}^o$  transition, we have  $g_J(2F_{5/2}^o) = 6/7$  and  $g_J(4I_{9/2}^o) = 8/11$ . Using the values of  $A/g_I$  given in Table IV for the clock states we obtain after simple transformations the frequency shift for the  $4I_{9/2}^o(F=5) - 2F_{5/2}^o(F=3)$  transition,

$$|\Delta\nu| = \frac{|\Delta E^{(2)}(4I_{9/2}^o) - \Delta E^{(2)}(2F_{5/2}^o)|}{h} \approx 2.6 g_I \frac{\text{kHz}}{(\text{mT})^2} B^2.$$

Given  $B = 10 \mu\text{T}$ , putting  $g_I = 1$ , and using  $\nu_{\text{clock}} \approx 4.8 \times 10^{14}$  Hz we arrive at the estimate for the  $\text{Cf}^{15+}$  fractional clock shift:

$$\frac{|\Delta\nu|}{\nu_{\text{clock}}} \approx 5 \times 10^{-16}. \quad (23)$$

As follows from Eq. (22), for the  $4I_{9/2}^o(F=4) - 2F_{5/2}^o(F=2)$  transition we will get exactly the same frequency shift  $\Delta\nu$  as for the  $4I_{9/2}^o(F=5) - 2F_{5/2}^o(F=3)$  transition in absolute value but with the opposite sign. Thus, an averaging of the quadratic Zeeman shifts over these two transitions will lead to complete cancellation of this effect.

Similarly, the  $\text{Cf}^{17+}$  clock  $6p_{1/2} - 5f_{5/2}$  transition frequency shift is

$$|\Delta\nu| = \frac{1}{h} \left| \Delta E^{(2)}(6p_{1/2}) - \Delta E^{(2)}(5f_{5/2}) \right|. \quad (24)$$

Taking into account that  $A(6p_{1/2})$  is two orders of magnitude larger than  $A(5f_{5/2})$  we can neglect  $\Delta E^{(2)}(6p_{1/2})$  compared to  $\Delta E^{(2)}(5f_{5/2})$ , arriving at

$$|\Delta\nu| \approx \frac{|\Delta E^{(2)}(5f_{5/2})|}{h} \approx 6.3 \frac{\text{kHz}}{(\text{mT})^2} g_I B^2. \quad (25)$$

Substituting  $g_I = 1$  and  $B = 10 \mu\text{T}$  to Eq. (25) and using  $\nu_{\text{clock}} \approx 6.1 \times 10^{14}$  Hz, we obtain for  $\text{Cf}^{17+}$ ,

$$\frac{|\Delta\nu|}{\nu_{\text{clock}}} \approx 1.0 \times 10^{-15}. \quad (26)$$

At a small magnetic field of  $\sim 10 \mu\text{T}$ , the fractional clock shift is with  $\sim 10^{-15}$  non-negligible for both ions. We expect that at these low fields and provided sufficient

shielding, the magnetic field drifts can be reduced to a level of  $< 10$  pT over time scales of several minutes. This results in relative frequency shifts of the clock transition from the linear Zeeman effect below  $10^{-17}$ , which can be averaged to zero by probing pairs of  $\pm|m_F|$  states [42]. The change in the quadratic Zeeman effect is negligible at the  $10^{-20}$  level.

To determine the quadratic shift precisely, the magnetic field needs to be known with a high accuracy. The difference of frequencies of the  $|F, m_F\rangle - |F', m'_F\rangle$  and  $|F, -m_F\rangle - |F', -m'_F\rangle$  hyperfine transitions will provide an accurate measurement of the  $B$  field and its potential fluctuation. However, in all cases a precise measurement of the nuclear magnetic moments is required to cancel the shift, which will require a measurement of the hyperfine structure and improving the accuracy of the  $A/g_I$  theoretical calculations. Alternatively, the  $g$ -factors can be determined using a co-trapped logic ion as a reference [44], such as  $\text{Be}^+$  with a well-known  $g$ -factor at the ppm level [45]. The logic ion can also serve directly as a probe for the magnetic field during clock operation.

As we discussed above, we can eliminate the electric quadrupole shift by averaging transitions involving different Zeeman components. The same approach can be applied, when  $F = I \pm 1/2$  to eliminate the quadratic Zeeman shift. This method works also for cancellation of the linear and quadratic Zeeman shifts in more general cases [2, 35].

## V. CONCLUSION

To conclude, we have carried out a systematic study of the  $\text{Cf}^{15+}$  and  $\text{Cf}^{17+}$  properties needed for the devel-

opment of optical clocks with these ions using the hybrid approach that combines the CI and coupled cluster methods. We analysed a number of systematic effects (such as the electric quadrupole-, micromotion-, and quadratic Zeeman shifts of the clock transitions) that affect the accuracy and stability of the optical clocks. We also calculated the hfs magnetic dipole constants of the clock states and the BBR shifts of the clock transitions. Based on our calculation and experimental progress in cooling and trapping HCIs [2, 3] we conclude that both the  $\text{Cf}^{15+}$  and  $\text{Cf}^{17+}$  ions are good candidates for optical clock. It was demonstrated earlier that such clocks would have very high sensitivity to a variation of the fine-structure constant [16, 17].

## ACKNOWLEDGMENTS

This work was supported in part by U.S. Office of Naval Research, award number N00014-17-1-2252. S.G.P., A.I.B., M.G.K., and I.I.T. acknowledge support by the Russian Science Foundation under Grant No. 19-12-00157. P.O.S acknowledges support from the Max-Planck-Riken-PTB-Center for Time, Constants and Fundamental Symmetries and the Deutsche Forschungsgemeinschaft (DFG, German Research Foundation) through SCHM2678/5-1, and Germany's Excellence Strategy ?? EXC-2123/1 QuantumFrontiers 390837967.

- 
- [1] L. Schmöger, O. O. Versolato, M. Schwarz, M. Kohlen, A. Windberger, B. Piest, S. Feuchtenbeiner, J. Pedregosa-Gutierrez, T. Leopold, P. Micke, A. K. Hansen, T. M. Baumann, M. Drewsen, J. Ullrich, P. O. Schmidt, and J. R. Crespo López-Urrutia, *Science* **347**, 1233 (2015).
  - [2] M. G. Kozlov, M. S. Safronova, J. R. Crespo López-Urrutia, and P. O. Schmidt, *Rev. Mod. Phys.* **90**, 045005 (2018).
  - [3] P. Micke, T. Leopold, S. A. King, E. Benkler, L. J. Spieß, L. Schmöger, M. Schwarz, J. R. Crespo López-Urrutia, and P. O. Schmidt, *Nature (London)* **578**, 60 (2020).
  - [4] S. Schiller, *Phys. Rev. Lett.* **98**, 180801 (2007).
  - [5] J. C. Berengut, V. A. Dzuba, and V. V. Flambaum, *Phys. Rev. Lett.* **105**, 120801 (2010).
  - [6] A. Derevianko, V. A. Dzuba, and V. V. Flambaum, *Phys. Rev. Lett.* **109**, 180801 (2012).
  - [7] V. A. Dzuba, A. Derevianko, and V. V. Flambaum, *Phys. Rev. A* **86**, 054501 (2012).
  - [8] V. A. Dzuba, A. Derevianko, and V. V. Flambaum, *Phys. Rev. A* **87**, 029906 (2013).
  - [9] A. Derevianko and M. Pospelov, *Nature Phys.* **10**, 933 (2014).
  - [10] Y. V. Stadnik and V. V. Flambaum, *Phys. Rev. Lett.* **115**, 201301 (2015).
  - [11] Y. V. Stadnik and V. V. Flambaum, *Phys. Rev. A* **94**, 022111 (2016).
  - [12] L. Schmöger, M. Schwarz, T. M. Baumann, O. O. Versolato, B. Piest, T. Pfeifer, J. Ullrich, P. O. Schmidt, and J. R. Crespo López-Urrutia, *Rev. Sci. Instrum.* **86**, 103111 (2015).
  - [13] M. Schwarz, O. O. Versolato, A. Windberger, F. R. Brunner, T. Ballance, S. N. Eberle, J. Ullrich, P. O. Schmidt, A. K. Hansen, A. D. Gingell, M. Drewsen, and J. R. Crespo López-Urrutia, *Rev. Sci. Instrum.* **83**, 083115 (2012).
  - [14] T. Leopold, S. A. King, P. Micke, A. Bautista-Salvador, J. C. Heip, C. Ospelkaus, J. R. Crespo López-Urrutia, and P. O. Schmidt, *Rev. Sci. Instrum.* **90**, 073201 (2019).
  - [15] P. Micke, J. Stark, S. A. King, T. Leopold, T. Pfeifer, L. Schmöger, M. Schwarz, L. J. Spieß, P. O. Schmidt, and J. R. Crespo López-Urrutia, *Rev. Sci. Instrum.* **90**, 065104 (2019).



- [16] J. C. Berengut, V. A. Dzuba, V. V. Flambaum, and A. Ong, *Phys. Rev. Lett.* **109**, 070802 (2012).
- [17] V. A. Dzuba, M. S. Safronova, U. I. Safronova, and V. V. Flambaum, *Phys. Rev. A* **92**, 060502 (2015).
- [18] M. G. Kozlov, S. G. Porsev, and V. V. Flambaum, *J. Phys. B* **29**, 689 (1996).
- [19] V. M. Shabaev, I. I. Tupitsyn, and V. A. Yerokhin, *Phys. Rev. A* **88**, 012513 (2013).
- [20] I. I. Tupitsyn, M. G. Kozlov, M. S. Safronova, V. M. Shabaev, and V. A. Dzuba, *Phys. Rev. Lett.* **117**, 253001 (2016).
- [21] V. A. Dzuba, V. V. Flambaum, and M. G. Kozlov, *Phys. Rev. A* **54**, 3948 (1996).
- [22] M. S. Safronova, M. G. Kozlov, W. R. Johnson, and D. Jiang, *Phys. Rev. A* **80**, 012516 (2009).
- [23] M. G. Kozlov, *Int. J. Quant. Chem.* **100**, 336 (2004).
- [24] S. G. Porsev and A. Derevianko, *Phys. Rev. A* **73**, 012501 (2006).
- [25] M. S. Safronova, V. A. Dzuba, V. V. Flambaum, U. I. Safronova, S. G. Porsev, and M. G. Kozlov, *Phys. Rev. A* **90**, 042513 (2014).
- [26] M. S. Safronova, V. A. Dzuba, V. V. Flambaum, U. I. Safronova, S. G. Porsev, and M. G. Kozlov, *Phys. Rev. A* **90**, 052509 (2014).
- [27] C. C. Cannon and A. Derevianko, *Phys. Rev. A* **69**, 030502 (2004).
- [28] A. Derevianko and S. G. Porsev, *Phys. Rev. A* **71**, 032509 (2005).
- [29] N. F. Ramsey, *Molecular Beams* (Oxford Univ. Press, London, 1956).
- [30] W. Itano, *J. Res. Natl. Inst. Stand. Technol.* **105**, 829 (2000).
- [31] P. Dubé, A. Madej, J. Bernard, L. Marmet, J.-S. Boulanger, and S. Cundy, *Phys. Rev. Lett.* **95**, 033001 (2005).
- [32] H. S. Margolis, G. P. Barwood, G. Huang, H. A. Klein, S. N. Lea, K. Szymaniec, and P. Gill, *Science* **306**, 1355 (2004).
- [33] M. Chwalla, J. Benhelm, K. Kim, G. Kirchmair, T. Monz, M. Riebe, P. Schindler, A. Villar, W. Hänsel, C. Roos, R. Blatt, M. Abgrall, G. Santarelli, G. Rovera, and P. Laurent, *Phys. Rev. Lett.* **102**, 023002 (2009).
- [34] A. A. Madej, P. Dubé, Z. Zhou, J. E. Bernard, and M. Gertsch, *Phys. Rev. Lett.* **109**, 203002 (2012).
- [35] P. Dubé, A. A. Madej, Z. Zhou, and J. E. Bernard, *Phys. Rev. A* **87**, 023806 (2013).
- [36] R. Shaniv, N. Akerman, and R. Ozeri, *Phys. Rev. Lett.* **116**, 140801 (2016).
- [37] M. G. Kozlov and S. G. Porsev, *Eur. Phys. J. D* **5**, 59 (1999).
- [38] M. S. Safronova, W. R. Johnson, and A. Derevianko, *Phys. Rev. A* **60**, 4476 (1999).
- [39] D. J. Berkeland, J. D. Miller, J. C. Bergquist, W. M. Itano, and D. J. Wineland, *J. Appl. Phys.* **83**, 5025 (1998).
- [40] J. Keller, H. L. Partner, T. Burgermeister, and T. E. Mehlstäubler, *J. Appl. Phys.* **118**, 104501 (2015).
- [41] N. Edelstein and D. G. Karraker, *J. Chem. Phys.* **62**, 938 (1975).
- [42] J. E. Bernard, L. Marmet, and A. A. Madej, *Opt. Commun.* **150**, 170 (1998).
- [43] G. Breit and I. Rabi, *Phys. Rev.* **28**, 2082 (1931).
- [44] T. Rosenband, P. O. Schmidt, D. B. Hume, W. M. Itano, T. M. Fortier, J. E. Stalnaker, K. Kim, S. A. Diddams, J. C. J. Koelemeij, J. C. Bergquist, and D. J. Wineland, *Phys. Rev. Lett.* **98**, 220801 (2007).
- [45] D. J. Wineland, J. J. Bollinger, and W. M. Itano, *Phys. Rev. Lett.* **50**, 628 (1983).